Quantum chemical study of the mechanism of oxidation of $C_{15}H_9$ by atomic oxygen

Galiya Galimova[1], *Valeriy* Azyazov[1,2], *Alexander* Mebel[1,3*]

[1]Samara University, Samara, 443086, Russia
[2]Lebedev Physical Institute, Samara, 443011, Russia
[3]Department of Chemistry and Biochemistry, Florida International University, Miami, FL 33199, USA

Abstract. An important environmental problem related to the use of fossil fuels is the formation of soot during combustion. Mechanisms of soot oxidation, which alleviates its emission into the environment, are not fully understood. The reaction of O with a radical $C_{15}H_9$ may play an important role in combustion. In this article, the $C_{15}H_9$ molecule was chosen as a model of soot surface. The paper discusses various pathways resulting from the $C_{15}H_9$ + O reaction. Relative energies, frequencies and optimal geometries of the reactants, products, intermediates and transition states of the $C_{15}H_9$ + O reaction have been calculated using the quantum-chemical Gaussian and Molpro program packages. The reaction pathways leading to carbon monoxide CO elimination have been found and dscussed.

1 Introduction

One of the major harmful emissions occuring during combustion of hydrocarbon fuels is the emission of soot. Soot believed to be formed as aggregates of polycyclic aromatic hydrocarbons (PAH) [1]. The mechanisms of soot formation and destruction in hydrocarbon flames are extremely complex.

It is established that O_2, OH and atomic O are the major oxidizers of soot. Present kinetic combustion models, as a rule, describe soot oxidation as a result of collision between O_2, OH and O and the surface of soot particles. The reactions lead to degradation of soot when it eliminates a CO molecule.

The $C_{15}H_9$ molecule can serve as a model for a soot surface radical site produced by an H atom abstruction/elimination from barely reactive closed-shell soot surface. The purpose of the present study is to investigate the reaction pathways of $C_{15}H_9$ + O, to find the optimal geometry of the structures obtained, and to calculate vibrational frequencies and energies for all the considered reactants, products, intermediates and transition states, which can be utilized in future calculations of reaction rate constants and kinetic modeling of soot oxidation.

* Corresponding author: mebela@fiu.edu

2 Theoretical methods

Ab initio electronic structure calculations have been applied to investigate possible products of the $C_{15}H_9$ + O reactions and to find the reaction paths that are energetically feasible for this reaction. The geometries of various species (reactants, products, intermediates, and transition states) involved in the $C_{15}H_9$ + O reactions were optimized using the hybrid density functional B3LYP method with the 6-311G** basis set. The same B3LYP/6-311G** approach was used to compute vibrational frequencies and zero-point energy (ZPE) corrections.

Next, the G3(MP2,CC)//B3LYP version [2] of the original Gaussian 3 (G3) scheme for high-level single-point calculations was applied to obtain more accurate energies of all species. The B3LYP and MP2 calculations were performed using the Gaussian 09 program package [3], whereas the MOLPRO 2010 program package [4] was employed for RHF-RCCSD(T) calculations.

3 Results and discussion

We consider the reaction mechanism of the O atom with a five-member ring radical embedded in a sheet of six-member rings, like at the edge of a graphene sheet or a large PAH molecule. The oxidation process with atomic oxygen is emulated by the O reactions with $C_{15}H_9$ radicals made from three six-member and one five-member rings. Figures 1 and 2 show two different possible modes of embedding represented by two $C_{15}H_9$ isomers, (A) and (B). Isomer (A) has the embedded five-member ring sharing two edges (C-C bonds) with other six-member rings, whereas in (B) three C-C bonds in the five-member ring are shared with the six-member rings and the embedding is deeper. The computed potential energy diagrams for the reactions of these isomers with atomic oxygen are also shown in Figs. 1 and 2. While the general mechanistic features of the $C_{15}H_9$(A) + O and the $C_{15}H_9$(B) + O reactions are similar, the details and the energetics differ substantially.

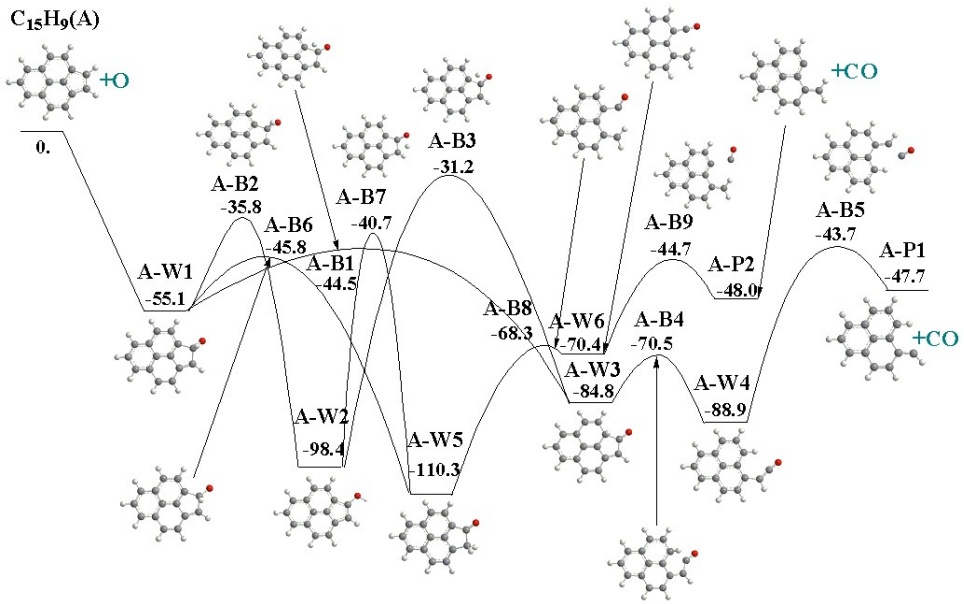

Fig. 1. Potential energy diagram for the $C_{15}H_9$(A) + O reaction calculated at the G3(MP2,CC)//B3LYP/6-311G(d,p) level of theory. All relative energies are given in kcal/mol with respect to the initial reactants.

Figure 1 shows the $C_{15}H_9$(A) + O reaction, where barrierless O addition to the five-member ring in the entrance channel is 55.1 kcal/mol exothermic and forms the intermediate A_W1. A_W1 can evolve to $C_{14}H_9$ + CO (A_P1) by isomerization and decarbonylation via the following pathways: A_W1 → A_B1 (A_B2 → A_W2 → A_B3) → A_W3 → A_B4 → A_W4 → A_B5 → A_P1. These channels involve either direct formation of A_W3 by H migration from the C atom attacked by O to the *ortho* C atom common for the five- and six-member rings or via a two-step process with an H shift from carbon to oxygen forming A_W2 followed by a second H shift from O to *ortho* C. A_W3 then features the five-member ring opening forming A_W4; the latter eliminates the CO group and produces $C_{14}H_9$ + CO (A_P1) residing 47.7 kcal/mol below the initial reactants. The critical barriers on these pathways appeared to be A_B3 or A_B5, which lie 31.2 and 43.7 kcal/mol lower in energy than the $C_{15}H_9$(A) + O reactants, respectively.

The alternative reaction channel is A_W1 → A_B6 (A_B2 → A_W2 → A_B7) → A_W5 → A_B8 → A_W6 → A_B9 → A_P2. The pathways in this channel involve either direct formation of A_W5 by H migration from the attacked carbon to the *ortho* C atom exclusively belonging to the five-member ring or via a two-step process through the intermediate A_W2. A_W5 then features opening of the ring and formation of A_W6; the latter eliminates the CO group and produces $C_{14}H_9$ + CO (A_P2), 48.7 kcal/mol below the reactants. The critical barriers on these pathways are found at A_B2 and A_B7 residing 35.8 and 40.7 kcal/mol below the initial reactants. The difference in the structures of the A_P1 and A_P2 products is that in the former the radical is located on the side chain, while in the latter the radical is on the six-member ring. In both mechanisms, the five-member ring of $C_{15}H_9$ is annihilated in the reaction of $C_{15}H_9$(A) with atomic oxygen producing radicals consisting of only three aromatic six-member rings plus CO. Calculations of rate constants and product branching ratios are planned in the future to quantify the competition between the two ways of decarbonylation.

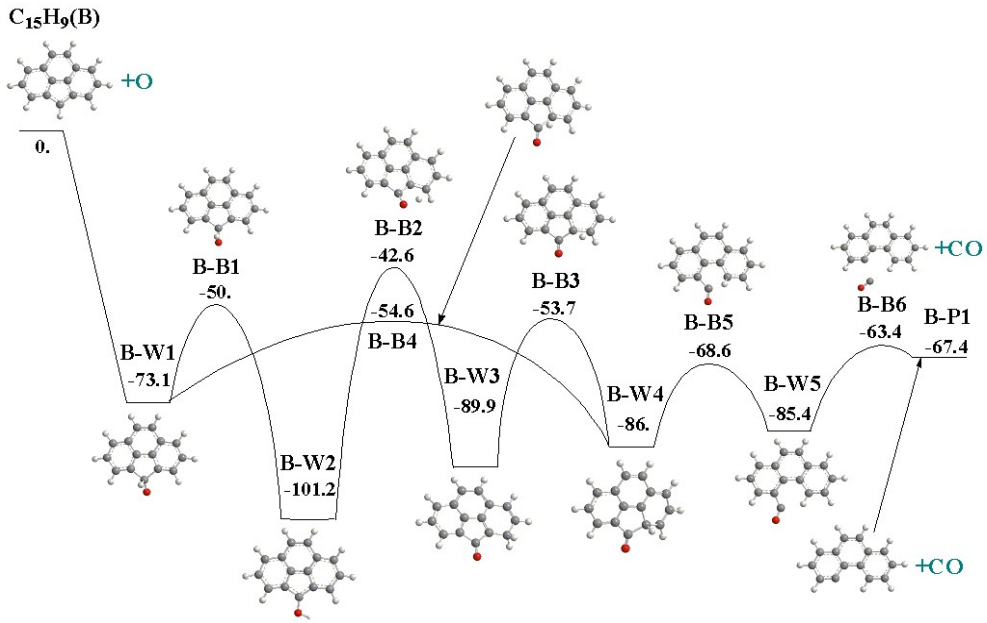

Fig. 2. Potential energy diagram for the $C_{15}H_9$(B) + O reaction calculated at the G3(MP2,CC)//B3LYP/6-311G(d,p) level of theory. All relative energies are given in kcal/mol with respect to the initial reactants.

In the $C_{15}H_9$(B) + O reaction, the initial association step forming B_W1 is 73.1 kcal/mol exothermic. The decarbonylation process of B_W1 producing $C_{14}H_9$ + CO proceeds via the B_W2, B_W3, and B_W4 intermediates. B_W4 can be formed from B_W1 either in one step via B_B4, by 1,2-H migration to the *ortho* carbon with respect to the attacked C atom, or via a three-step pathway B_W1 → B_B1 → B_W2 → B_B2 → B_W3 → B_B3 → B_W4 involving consecutive 1,2-H shift from C to O, 1,4-H migration from O to the C atom in the neighboring six-member ring, and 1,2-H shift back to the *ortho* carbon atom. Here, the one-step process is clearly preferable since the transition state B_B4, 54.6 kcal/mol below the reactants, lies 12.0 kcal/mol lower in energy than B_B2. Opening of the five-member ring in B_W4 produces B_W2 via a relatively low barrier of 17.4 kcal/mol at B_B5 residing 68.6 kcal/mol below the reactants. Finally, B_W5 eliminates the CO group and produces the 4-phenanthrenyl radical $C_{14}H_9$ (B_P1). The critical transition state for the most favorable decarbonylation pathway is B_B4.

Conclusion

The most likely pathways of the reaction $C_{15}H_9$ + O were considered. The optimal geometry of the structures, vibrational frequencies, energies of products, reagents, intermediates and transition states that are involved in the $C_{15}H_9$ + O reaction were calculated.

The reaction pathways leading to the expulsion of the CO molecule were also determined. In the future, the calculated energetic and molecular parameters will be used to calculate pressure- and temperature-dependent rate constants for the oxidation of five-member rings with atomic oxygen on the surface of soot particles and large PAHs using the RRKM-Master Equation approach.

Acknowledgments

The work was supported by the Ministry of Education and Science of the Russian Federation under Grant no.14.Y26.31.0020 to Samara University.

References

1. H. Richter, J.B. Howard, Formation of polycyclic aromatic hydrocarbons and their growth to soot - a review of chemical reaction pathways, Prog. Energ. Combust. Sci. 26 565 (2000)
2. M. J. Frisch, G.W. Trucks, H.B. Schlegel, Gaussian 09, revision B.01. Wallingford, CT: Gaussian, Inc (2010)
3. H. J. Werner, P. J. Knowles, R. Lindh, MOLPRO, version 2015.1, a package of ab initio programs. Available at: http://www.molpro.net (2015)
4. Y. Georgievskii, J.A. Miller, M.P. Burke, and S. J. Klippenstein, Reformulation and solution of the master equation for multiple-well chemical reactions. J. Phys. Chem. A 117 12146 (2013)